

Enhancement of thermoelectric efficiency in granular Co-Cu thin films from spin-dependent scattering

Cite as: Appl. Phys. Lett. **116**, 042401 (2020); <https://doi.org/10.1063/1.5129334>

Submitted: 27 September 2019 . Accepted: 04 January 2020 . Published Online: 27 January 2020

Z. Yan, B. Wang, X. W. Lv, W. B. Sui, J. W. Cao , H. G. Shi, M. S. Si, D. Z. Yang , and D. S. Xue



View Online



Export Citation



CrossMark

ARTICLES YOU MAY BE INTERESTED IN

[Toward attosecond control of electron dynamics in two-dimensional materials](#)

Applied Physics Letters **116**, 043101 (2020); <https://doi.org/10.1063/1.5135599>

[A 30-nm thick integrated hafnium zirconium oxide nano-electro-mechanical membrane resonator](#)

Applied Physics Letters **116**, 043501 (2020); <https://doi.org/10.1063/1.5134856>

[Achieving high-resolution of 21nm for STED nanoscopy assisted by CdSe@ZnS quantum dots](#)

Applied Physics Letters **116**, 041101 (2020); <https://doi.org/10.1063/1.5133427>



Lock-in Amplifiers

Zurich Instruments

Watch the Video

Enhancement of thermoelectric efficiency in granular Co-Cu thin films from spin-dependent scattering

Cite as: Appl. Phys. Lett. **116**, 042401 (2020); doi: 10.1063/1.5129334

Submitted: 27 September 2019 · Accepted: 4 January 2020 ·

Published Online: 27 January 2020



View Online



Export Citation



CrossMark

Z. Yan, B. Wang, X. W. Lv, W. B. Sui, J. W. Cao,  H. G. Shi, M. S. Si, D. Z. Yang,  and D. S. Xue^{a)}

AFFILIATIONS

Key Laboratory for Magnetism and Magnetic Materials of Ministry of Education, Lanzhou University, Lanzhou 730000, China

^{a)} Authors to whom correspondence should be addressed: yangdezh@lzu.edu.cn and xueds@lzu.edu.cn

ABSTRACT

In contrast to traditional concepts that eliminate magnetic impurities to achieve larger thermoelectric efficiencies, we report an enhanced thermoelectric efficiency for Cu through doping with the magnetic impurity Co. With doping concentrations from 15% to 30%, the amplitude of the Seebeck coefficient increases from 1.90 $\mu\text{V}/\text{K}$ up to 16.3 $\mu\text{V}/\text{K}$, which greatly enhances the thermoelectric efficiency (i.e., power factor). Measuring the magnetoresistance and magnetothermoelectric powers at different temperatures indicates that the enhancement of thermoelectric efficiency is a result of spin-dependent scattering from Co nanoparticles, which are less sensitive to the superparamagnetic transitions. Our finding illustrates a path for the use of nanomagnets to develop potential thermoelectric materials.

Published under license by AIP Publishing. <https://doi.org/10.1063/1.5129334>

Thermoelectric (TE) devices are a class technology that directly converts heat to electrical energy. Compared with conventional energy-conversion technologies, TE materials have intrinsic advantages, such as sustainability, availability, reliability, and predictability.¹ However, very low TE efficiency still inhibits their practical applications. The efficiency of TE materials is usually determined from the power factor $PF = \alpha^2/\rho$ and the dimensionless figure of merit $ZT = \alpha^2 T/\rho\kappa$, where α is the Seebeck coefficient (i.e., thermopower), T is the temperature in Kelvin, ρ is the electrical resistivity, and κ is the thermal conductivity that includes both the charge-carrier thermal conductivity κ_E and the lattice conductivity κ_L . Experiments and theories have shown that values of PF and ZT could be greatly enhanced by improving the phonon and/or electron transport. For example, interface structure design^{2,3} or anharmonicity⁴⁻⁷ is important for phonon transport, and band structure engineering⁸ or doping modulation⁹ is important for electron transport.

Recently, the emerging role of spin-based technologies holds great promise for developing next generation high-performance TE materials.¹⁰ Inducing the spin Seebeck effect¹¹ doped with strong spin-orbit interacting metallic nanoparticles (Pt or Au) in ferromagnetic metals (Ni and MnBi) enhances the transverse ZT by an order of magnitude due to improving α while limiting ρ .¹² The large α in $\text{Na}_x\text{Co}_2\text{O}_4$ has been applied as a contribution to the spin entropy of charge carriers.¹³ Recently, Zhao *et al.* introduced

ferromagnetic Co nanoparticles into the TE semiconductor $\text{Ba}_{0.3}\text{In}_{0.3}\text{Co}_4\text{Sb}_{12}$.¹⁴ Despite a doping concentration of only 0.2%, the ZT sharply increased from approximately 1.3 to 1.8. A similarly enhanced ZT was also observed through the doping of Fe or Ni nanoparticles, indicating that this phenomenon can be considered as a general property. They ascribed the enhanced ZT , at least in part, as a result of fluctuating superparamagnetic moments due to selective scattering. However, the enhanced ZT in their experiments appears unrelated to the blocking temperature (T_B) of the magnetic transition from ferromagnet to superparamagnet. Thus, the explanation behind ZT enhancement induced by nanomagnets is still incomplete. Further investigating this effect in a more ideal system will help to improve current understandings.¹⁵

In this work, we selected granular Co-Cu thin films to investigate the enhancement of the ZT . Similar to Zhao's results in semiconductor TE materials,¹⁴ we observed more obvious enhancements in metal TE materials. When the Co concentration increases from 15% to 30%, the ZT is enhanced by more than an order of magnitude. To understand the physics of the enhanced ZT , the electrical and thermal spin transport behaviors of the Co-Cu granular films at various temperatures were systematically measured. The data show that the spin-dependent thermal transport is closely related to the magnetoresistance (MR) behaviors, even when above T_B . This indicates that the ZT enhancement may originate from spin-dependent scattering rather than

superparamagnetic selective scattering. These results provide a route to find high ZT TE materials.

Granular Co-Cu thin films were fabricated on the corning glass using a Co-Cu co-sputtering method under a high vacuum of 3×10^{-5} Pa and the Ar pressure of 0.3 Pa during deposition. The composition of Co-Cu was controlled by adjusting the deposition rates of Co and Cu, and the thicknesses of Co-Cu alloy thin films were controlled by adjusting the deposition time. In this work, the thicknesses of all samples were fixed at 300 nm. The samples were rotated during the sputtering process to maintain the uniformity of the Co-Cu composition. The magnetic properties of the Co-Cu thin films were measured using a superconducting quantum interference device (SQUID). The superparamagnetic transition in Co-Cu alloy thin films is shown in Fig. S1. The microstructure of Co nanoparticles is confirmed using a high resolution transmission electron microscope (HRTEM) in Fig. S2. The structures of Co-Cu thin films were characterized by X-ray diffraction (XRD) in Fig. S3 of the [supplementary material](#). The electrical and thermal transport measurements were carried out using a physical property measurement system (PPMS). The thermopower measurements were performed using the continuous mode PPMS protocol. The magnitude of the ΔT applied in this work is several Kelvin.

We performed zero field-cooling (ZFC) and field-cooling (FC) measurements to determine the T_B of the granular Co-Cu thin films. For ZFC processes, the samples were cooled without a magnetic field from 300 to 5 K and then heated back to 300 K under a magnetic field of 5 mT while simultaneously measuring the magnetization to capture the magnetization vs temperature ($M-T$) curves. For FC processes, the same procedure was performed, but the beginning cooling process included the application of a small magnetic field. The small magnetic field could avoid the nonlinearity effect.¹⁶ Figure 1 shows the FC and ZFC curves for the granular Co-Cu thin films with different Co compositions. An obvious difference between the ZFC and FC curves was observed at low temperatures.^{17,18} Below T_B , the ZFC and FC curves diverge significantly, indicating that the granular Co-Cu thin films were in a ferromagnetic state. Above T_B , the ZFC and FC curves gradually coincide, indicating that the granular Co-Cu thin films became superparamagnetic, also in Fig. S1. When the Co composition increased from 15% to 30%, the T_B gradually increased, as shown in Figs. 1(a)–1(d). This indicates that the superparamagnetic transition T_B gradually increases with the increasing Co concentration. The increased T_B at higher Co concentrations demonstrates that the larger energy barrier should be overcome to flip the magnetic moments of the Co nanoparticles due to the increased Co particle volumes. This is consistent with the HRTEM images in Fig. S2 of the [supplementary material](#). As the Co concentration increases, the average volume of Co nanoparticles gradually increases.

Figure 2 shows the typical in-plane hysteresis loops of the granular $\text{Co}_{25}\text{Cu}_{75}$ thin film. When T (150 K) is smaller than T_B (160 K), the hysteresis loop in Fig. 2(a) presents a prominent ferromagnetic behavior with a coercivity of 1.6 mT. When $T > T_B$, as shown in Figs. 2(b) and 2(c), the hysteresis loops exhibit superparamagnetic behaviors, where both the coercivity and remanence magnetization are zero. In the small and large magnetic field ranges [insets of Figs. 2(b) and 2(c), respectively], the superparamagnetic hysteresis loops can be well fitted using the Langevin function,

$$M = M_S[\coth(mH/k_B T) - k_B T/mH], \quad (1)$$

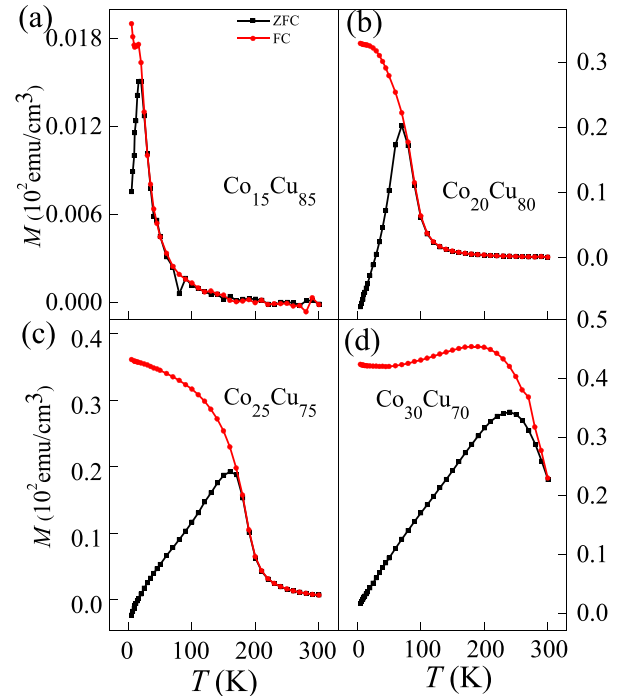


FIG. 1. Zero-field-cooling (ZFC) and field-cooling (FC) magnetization vs temperature ($M-T$) for granular Co-Cu thin films with different Co concentrations. The divergence of FC and ZFC shows the superparamagnetic block temperature T_B for the superparamagnetic transition.

where M_S is the saturation magnetization, m is the average magnetic moment of the Co particles, k_B is Boltzmann's constant, and H is the magnetic field. The fit yields a Co-Cu thin film M_S of 1.27×10^2 emu/cm³ and an average magnetic moment of Co particles m of 2.67×10^{-19} Am². Considering that the magnetic moment of Co

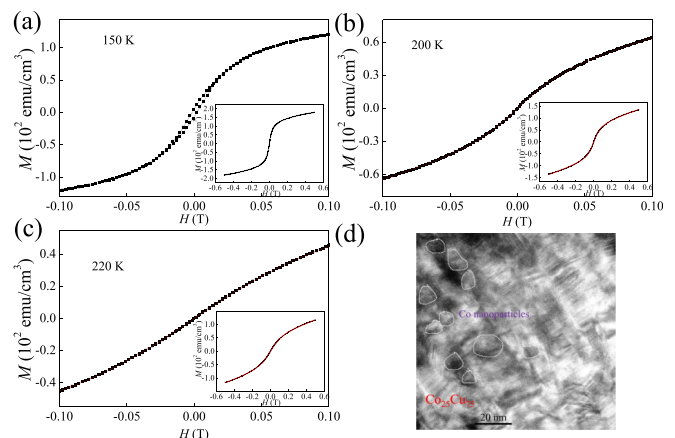


FIG. 2. The in-plane hysteresis loops for $\text{Co}_{25}\text{Cu}_{75}$ at (a) 150 K, (b) 200 K, and (c) 220 K. The red lines for 200 and 220 K are the fitting results using the Langevin function. The inset figures are the hysteresis loops at the same temperature, but over a larger magnetic field range. (d) The Co nanoparticles observed by HRTEM.

atoms is $I_s = 1.42 \times 10^6$ A/m, we can use m to calculate the average volume of Co nanoparticles $V = m/I_s = 1.88 \times 10^2$ nm³. For simplicity, if we assume that the Co nanoparticle is spherical, then the volume of the nanoparticle with diameter D is $V = \frac{1}{6}\pi D^3$. The average diameter D of Co nanoparticles is $D = (6V/\pi)^{1/3} = 7.10$ nm. The fitting value D is consistent with the average diameter of Co nanoparticles of Co₂₅Cu₇₅ measured by HRTEM in Fig. 2(d).

Figure 3(a) shows ρ as a function of T for the Co-Cu thin films with different Co concentrations. For all samples, the ρ increases with higher T , demonstrating a stronger metal behavior.¹⁹ At a specified temperature, ρ gradually increases at higher Co concentrations. It is found that the ρ of Co-Cu is much larger than that of Cu. This is because Co is a magnetic impurity, and so the enhanced ρ stems from both impurity and magnetic scattering events, also shown in Fig. S4.

Figure 3(b) shows the dependence of α on T for Cu and Co-Cu thin films. It is noted that the amplitude of α is significantly enhanced

due to the doped magnetic impurity of Co. When T increases from 3 to 270 K, the α for Cu is positive and increases from 0.15 to 2.08 μ V/K. However, when Co is doped into Cu, such as Co₁₅Cu₈₅, α becomes negative and sharply decreases from -1.09 to -16.26 μ V/K. At $T = 270$ K, the amplitude of α for Co₁₅Cu₈₅ is nearly eight times larger than for Cu.

The power factor $PF = \alpha^2/\rho$ is calculated from the experimental values of ρ_{Cu} , ρ_{CoCu} , α_{Cu} , and α_{CoCu} in Figs. 3(a) and 3(b) as shown in Fig. 3(c). At $T = 270$ K, $PF = 2.10 \times 10^{-5}$ WK²/m for Cu, while $PF = 9.34 \times 10^{-4}$ WK²/m for Co₂₅Cu₇₅. Considering the elastic scattering in Co-Cu thin films, the κ_E and ρ can be described using the Wiedemann Franz law of $\kappa_E/\rho T = L_0$,^{20,21} where L_0 is the Lorenz number value of 2.45×10^{-8} V²/K² for a free electron system.^{22,23} Therefore, the ZT could be simply expressed as $ZT \approx \alpha^2/L_0$, where κ_L is assumed to be negligible. Compared with Cu, the value of ZT at room temperature for the Co-Cu thin films is enhanced by more than one order of magnitude due to the increased α . Our results directly support Zhao's work,¹⁴ who first introduced magnetic impurities into TE semiconductor materials to enhance the ZT , and extend available thermoelectric materials from semiconductors to metals.

The observed ZT enhancement in TE metals (as opposed to semiconductors) can further help simplify the conditions to find the physical mechanisms that lead to these enhancements. Compared with Co nanoparticles in TE semiconductors, doping Co nanoparticles into metals (Cu) provides a broad palette of doping concentrations, charge transfer effects, and elastic scattering effects. First, Cu and Co are nominally immiscible, where Co is present as distinct particles and not alloyed into the Cu matrix. In contrast to the narrow doping ranges for TE semiconductors, the Co concentration in Cu thin films can vary over a wide range to significantly tune T_B . Second, due to the absence of the metal-semiconductor contact in Co-Cu, the charge transfer effect that affects the TE properties can be completely neglected. Third, the dominant elastic scattering processes in granular Co-Cu thin films have shown that the Wiedemann-Franz law is valid over a wide temperature range.²¹⁻²⁴

We further analyze the mechanism for the nanomagnetic improvements to the TE efficiency. The values of α and ρ of bulk Co are -30.8 μ V/K²⁵ and 6.0 $\mu\Omega$ cm, respectively. The values of α and ρ of bulk Cu are 1.8 μ V/K²⁶ and 1.8 $\mu\Omega$ cm, respectively. If we simply estimate the α of the Co-Cu alloy using the Nordheim-Gorter rule, then α of Co₁₅Cu₈₅ is -10.2 μ V/K, which is much smaller than the measured value. This indicates that a coupling between Co and Cu plays an important role in the transport properties. Moreover, despite the large variations of T_B in our work, the thermal efficiency enhancement appears unrelated to the superparamagnetic transition temperature, as shown in the dotted lines of Fig. 3(c).

To find the coupling between Co and Cu, Fig. 4(a) shows the MR curves for Co₂₅Cu₇₅. With an increased magnetic field, the magnetic moments of the Co particles from the random distributions gradually align toward the magnetic field orientation, which yields a lower resistivity due to the giant magnetoresistance (GMR) effect.²⁷⁻²⁹ The large MR effect for the Co-Cu thin films can be understood that the conduction electrons in Cu are spin-dependent scattered by the Co particles.^{18,30} Figure 4(b) shows similar magnetothermoelectric powers (MTP), due to the spin-dependent α of Co. It is found that the spin-dependent thermal transport is closely related to electrical transport behaviors.^{26,31,32} The observation of the negative signs of α and $\Delta\alpha$ of

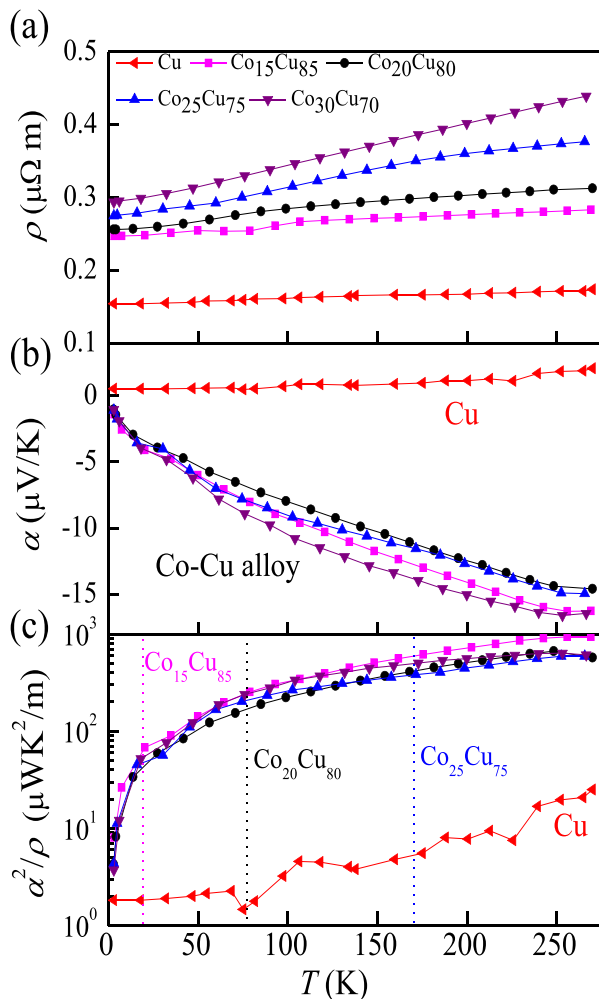


FIG. 3. The temperature dependence of the (a) resistivity ρ , (b) Seebeck coefficient α , and (c) power factor $PF = \alpha^2/\rho$ for the Co-Cu thin films with different Co concentrations. The dotted lines in (c) represent the superparamagnetic transition temperature T_B for the Co-Cu thin films with different Co compositions.

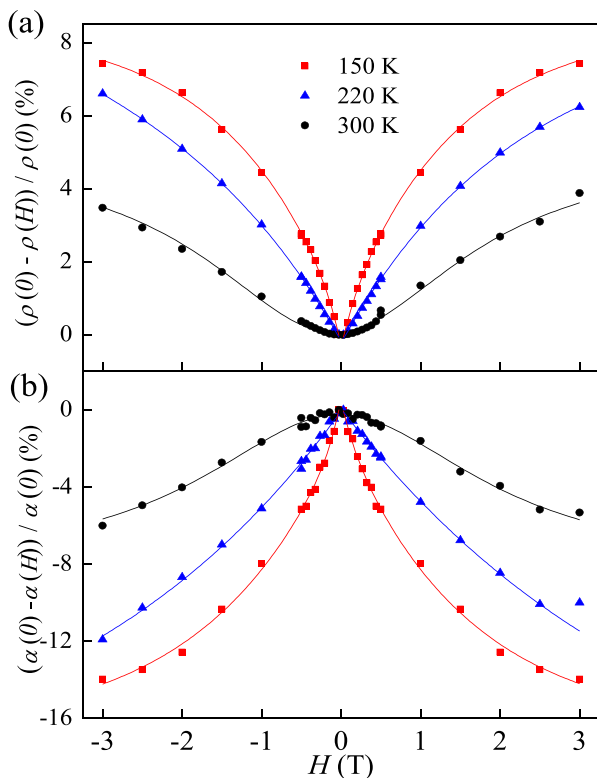


FIG. 4. The (a) magnetoresistance (MR) and (b) magnetothermoelectric power (MTP) curves for the granular $\text{Co}_{25}\text{Cu}_{75}$ thin film at different temperatures. The lines are guides to the eye.

the Co-Cu alloy as a function of magnetic field can be considered as direct evidence to confirm the spin dependent scattering. According to the Mott theory, α is a higher-order transport property and can be expressed through the derivative of the conductivity σ with respect to energy E , $\alpha = -\frac{\pi^2 k_B T}{3e} \left(\frac{\partial \ln \sigma(E)}{\partial E} \right)_{E_F}$. Owing to the hybridization between sp and d electrons, increasing the electron energy results in increasing the electron velocity, thus yielding both negative signs of α and $\Delta\alpha$. Based on the same mechanism, both the negative signs of α and $\Delta\alpha$ are also observed in other Co/Cu multilayers,^{26,33–35} Co-Ni/Cu multilayers,³⁶ $\text{Ni}_{81}\text{Fe}_{19}/\text{Cu}/\text{Co}$ spin valves,^{37–39} $\text{CoFe}/\text{Cu}/\text{CoFe}$ spin valves,⁴⁰ and $\text{FeNi}/\text{Cu}/\text{FeNi}$ spin valves.⁴¹ Thus, the more significant enhancement of the ZT in the Co-Cu alloy thin film than that in semiconductor materials can be explained by the large spin diffusion length in metal Cu.

More interestingly, the T_B for $\text{Co}_{25}\text{Cu}_{75}$ is only 160 K, but there are still significant MR and MTP effects at $T = 300$ K, as shown in Figs. 4(a) and 4(b), respectively. This demonstrates that the spin-dependent scattering is surprisingly valid even for Co particles in the superparamagnetic state. It is noted that even if $\text{Co}_{25}\text{Cu}_{75}$ is in a superparamagnetic state, the PFs (i.e., $T = 270$ K and $PF = 9.34 \times 10^{-4} \text{ WK}^2/\text{m}$) are still quite close to the value for Co/Cu multilayers from previous works,³² where the Co layers are in ferromagnetic states. The enhanced ZT due to spin-dependent scattering has been observed in granular Co-Ag,²⁶ granular Fe-Ag,²⁶ Co/Cu multilayers,^{26,33,35} Fe/Cr

multilayers,^{26,42} and spin valve multilayers,^{38,43,44} by controlling the magnetic configurations. However, the previous experiments mainly focused on ZT enhancements due to the changes in the magnetic configuration, while few experiments considered the nanomagnet effect, especially when in superparamagnetic states, to improve the TE efficiency.

In conclusion, we have shown an enhancement in the TE efficiency through doping magnetic impurities of Co into a Cu metal film, even when the Co particles are in superparamagnetic states. The continuous change in the TE efficiency at T_B excludes superparamagnetic scattering as the dominant mechanism for the enhanced TE efficiency. Further experiments show that the spin-dependent GMR and MTP effects for granular Co-Cu thin films are still valid, even above the T_B . This indicates that the spin-dependent transport plays an important role in the enhanced TE efficiency, even when the nanomagnets are in superparamagnetic states.

See the [supplementary material](#) for the Co nanoparticle microstructure and the structures, superparamagnetic transition, and scattering mechanisms of Co-Cu alloy thin films.

This work was supported by the NSFC of China (Grant Nos. 11774139, 11874189, and 11674143), PCSIRT (Grant No. IRT-16R35), and the Program for Science and Technology of Gansu Province (Grant No. 17YF1GA024).

REFERENCES

- L. E. Bell, *Science* **321**, 1457 (2008).
- P. Puneet, R. Podila, M. Karakaya, S. Zhu, J. He, T. M. Tritt, M. S. Dresselhaus, and A. M. Rao, *Sci. Rep.* **3**, 3212 (2013).
- B. Poudel, Q. Hao, Y. Ma, Y. Lan, A. Minnich, B. Yu, X. Yan, D. Wang, A. Muto, D. Vashaee, X. Chen, J. Liu, M. S. Dresselhaus, G. Chen, and Z. Ren, *Science* **320**, 634 (2008).
- J. Yang, L. Xi, W. Qiu, L. Wu, X. Shi, L. Chen, J. Yang, W. Zhang, C. Uher, and D. J. Singh, *npj Comput. Mater.* **2**, 15015 (2016).
- D. T. Morelli, V. Jovovic, and J. P. Heremans, *Phys. Rev. Lett.* **101**, 035901 (2008).
- H. Jin, O. D. Restrepo, N. Antolin, S. R. Boona, W. Windl, R. C. Myers, and J. P. Heremans, *Nat. Mater.* **14**, 601 (2015).
- T. Matsunaga, N. Yamada, R. Kojima, S. Shamoto, M. Sato, H. Tanida, T. Uruga, S. Kohara, M. Takata, P. Zalden, G. Bruns, I. Sergueev, H. C. Wille, R. P. Hermann, and M. Wuttig, *Adv. Funct. Mater.* **21**, 2232 (2011).
- Y. Pei, H. Wang, and G. J. Snyder, *Adv. Mater.* **24**, 6125 (2012).
- M. Zebarjadi, B. Liao, K. Esfarjani, M. Dresselhaus, and G. Chen, *Adv. Mater.* **25**, 1577 (2013).
- S. R. Boona, R. C. Myers, and J. P. Heremans, *Energy Environ. Sci.* **7**, 885 (2014).
- K. Uchida, S. Takahashi, K. Harii, J. Ieda, W. Koshibae, K. Ando, S. Maekawa, and E. Saitoh, *Nature* **455**, 778 (2008).
- S. R. Boona, K. Vandaele, I. N. Boona, D. W. McComb, and J. P. Heremans, *Nat. Commun.* **7**, 13714 (2016).
- Y. Wang, N. S. Rogado, R. J. Cava, and N. P. Ong, *Nature* **423**, 425 (2003).
- W. Zhao, Z. Liu, Z. Sun, Q. Zhang, P. Wei, X. Mu, H. Zhou, C. Li, S. Ma, D. He, P. Ji, W. Zhu, X. Nie, X. Su, X. Tang, B. Shen, X. Dong, J. Yang, Y. Liu, and J. Shi, *Nature* **549**, 247 (2017).
- S. R. Boona, *Nature* **549**, 169 (2017).
- A. Kundu, C. Upadhyay, and H. C. Verma, *Phys. Lett. A* **311**, 410 (2003).
- C. P. Bean and J. D. Livingston, *J. Appl. Phys.* **30**, S120 (1959).
- A. E. Berkowitz, J. R. Mitchell, M. J. Carey, A. P. Young, S. Zhang, F. E. Spada, F. T. Parker, A. Hutten, and G. Thomas, *Phys. Rev. Lett.* **68**, 3745 (1992).
- C. L. Chien, J. Q. Xiao, and J. S. Jiang, *J. Appl. Phys.* **73**, 5309 (1993).

- ²⁰J. Kimling, K. Nielsch, K. Rott, and G. Reiss, *Phys. Rev. B* **87**, 134406 (2013).
- ²¹A. D. Avery, S. J. Mason, D. Bassett, D. Wesenberg, and B. L. Zink, *Phys. Rev. B* **92**, 214410 (2015).
- ²²G. S. Kumar, G. Prasad, and R. O. Pohl, *J. Mater. Sci.* **28**, 4261 (1993).
- ²³H.-S. Kim, Z. M. Gibbs, Y. Tang, H. Wang, and G. J. Snyder, *APL Mater.* **3**, 041506 (2015).
- ²⁴L. Piraux, M. Cassart, J. S. Jiang, J. Q. Xiao, and C. L. Chien, *Phys. Rev. B* **48**, 638 (1993).
- ²⁵M. J. Laubitz and T. Matsumura, *Can. J. Phys.* **51**, 1247 (1973).
- ²⁶J. Shi, K. Pettit, E. Kita, S. S. P. Parkin, R. Nakatani, and M. B. Salamon, *Phys. Rev. B* **54**, 15273 (1996).
- ²⁷S. M. Thompson, *J. Phys. D* **41**, 093001 (2008).
- ²⁸M. N. Baibich, J. M. Broto, A. Fert, F. N. Van Dau, F. Petroff, P. Etienne, G. Creuzet, A. Friederich, and J. Chazelas, *Phys. Rev. Lett.* **61**, 2472 (1988).
- ²⁹G. Binasch, P. Grünberg, F. Saurenbach, and W. Zinn, *Phys. Rev. B* **39**, 4828 (1989).
- ³⁰J. Q. Xiao, J. S. Jiang, and C. L. Chien, *Phys. Rev. B* **46**, 9266 (1992).
- ³¹S. W. Chen, Z. L. Yang, Y. L. Zuo, M. S. Si, L. Xi, H. G. Shi, D. Z. Yang, and D. S. Xue, *J. Phys. D* **51**, 405302 (2018).
- ³²X. K. Hu, P. Krzysteczko, N. Liebing, S. Serrano-Guisan, K. Rott, G. Reiss, J. Kimling, T. Böhnert, K. Nielsch, and H. W. Schumacher, *Appl. Phys. Lett.* **104**, 092411 (2014).
- ³³L. Gravier, A. Fábíán, A. Rudolf, A. Cachin, J.-E. Wegrowe, and J.-P. Ansermet, *J. Magn. Magn. Mater.* **271**, 153 (2004).
- ³⁴L. Gravier, J.-E. Wegrowe, T. Wade, A. Fabian, and J.-P. Ansermet, *IEEE Trans. Magn.* **38**, 2700 (2002).
- ³⁵S. A. Baily, M. B. Salamon, and W. Oepts, *J. Appl. Phys.* **87**, 4855 (2000).
- ³⁶T. Böhnert, A. C. Niemann, A.-K. Michel, S. Bäßler, J. Gooth, B. G. Tóth, K. Neuróhr, L. Péter, I. Bakonyi, V. Vega, V. M. Prida, and K. Nielsch, *Phys. Rev. B* **90**, 165416 (2014).
- ³⁷X. M. Zhang, C. H. Wan, H. Wu, P. Tang, Z. H. Yuan, Q. T. Zhang, X. Zhang, B. S. Tao, C. Fang, and X. F. Han, *J. Appl. Phys.* **122**, 145105 (2017).
- ³⁸F. K. Dejene, J. Flipse, G. E. W. Bauer, and B. J. van Wees, *Nat. Phys.* **9**, 636 (2013).
- ³⁹F. K. Dejene, J. Flipse, and B. J. van Wees, *Phys. Rev. B* **86**, 024436 (2012).
- ⁴⁰S. Jain, D. D. Lam, A. Bose, H. Sharma, V. R. Palkar, C. V. Tomy, Y. Suzuki, and A. A. Tulapurkar, *AIP Adv.* **4**, 127145 (2014).
- ⁴¹H. Sato, S. Miya, Y. Kobayashi, Y. Aoki, H. Yamamoto, and M. Nakada, *J. Appl. Phys.* **83**, 5927 (1998).
- ⁴²E. Y. Tsybal, D. G. Pettifor, J. Shi, and M. B. Salamon, *Phys. Rev. B* **59**, 8371 (1999).
- ⁴³A. Slachter, F. L. Bakker, J.-P. Adam, and B. J. van Wees, *Nat. Phys.* **6**, 879 (2010).
- ⁴⁴A. Slachter, F. L. Bakker, and B. J. van Wees, *Phys. Rev. B* **84**, 020412 (2011).